

# Virtual Laboratory for Technology FES FY2018 Fourth Quarter Report

Phil Ferguson  
for the VLT members



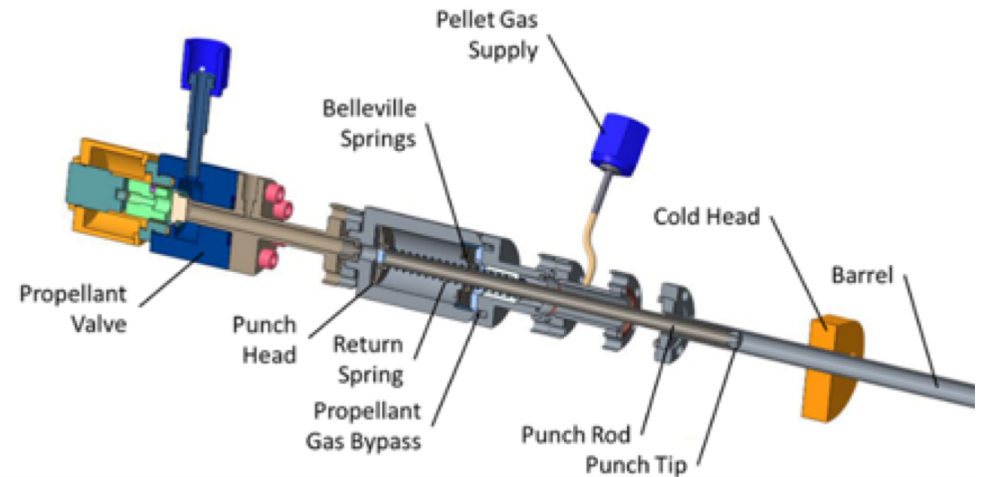
# Director's Corner

- The VLT, together with FES and ORNL, organized and participated in a workshop on a Fusion Prototypic Neutron Source (FPNS)
  - 33 members of the US fusion materials community, the Virtual Laboratory for Technology, and private industry met and discussed the possibility of the US exploring a FPNS
  - The source would be a potential near term, moderate cost, intermediate step to IFMIF/DONES/AFNS, not a replacement
  - Consensus was reached that the concept should be explored, and design ranges were identified
- The VLT is discussing an updated assessment of the Technology Readiness Levels (TRLs) of the fusion technology and nuclear science program
  - This would be a large effort, so won't be undertaken lightly
  - There is general agreement that TRLs is an effective way of communicating the status of the program, benchmarking progress over time (progression of TRLs), and identifying needs for future work
- This and future highlights will continue to cover research highlights from recent VLT publications and the main VLT research areas:
  - Magnet Systems; Heating & Current Drive; Plasma Fueling/ ELM Pacing/Disruption Mitigation
  - Plasma Facing Components; Plasma Materials Interactions; Structural Materials
  - Design/Systems studies; Power Handling; Fusion Safety; Fuel Cycle Research; Blanket Technology; Vacuum System

***If you have any questions on the information in this report, please don't hesitate to contact us.***

# Mechanical Punches for Argon/Neon Disruption Mitigation Pellets Developed and Delivered for the JET SPI

- Runaway electron mitigation in JET requires large shattered pellets of Argon/Neon that need a mechanical punch for dislodging the pellets.
- Pneumatically operated punches with sufficient force to break away 12 mm argon pellets survived 3 times the expected lifecycle in laboratory testing.
- Three final design prototypes were subjected to 270 worst case pulses (no pellet, full pressure impacts)
- Prototype punches survived with no fatigue cracking in welds or material interfaces. Two punches for JET SPI delivered in September.



One of three punches that survived lifecycle testing

Steve Meitner,  
Larry Baylor,  
Trey Gebhart, &  
Tam Ha

Work sponsored by  
DOE Office of Fusion  
Energy Sciences

# Gyrotron Power Reduction Caused by Reflections

## Scientific Achievement

- We have built a variable polarizer and reflecting mirror system for testing the effect of reflected power on the power output of a 1.5 MW, 110 GHz gyrotron.

## Significance and Impact

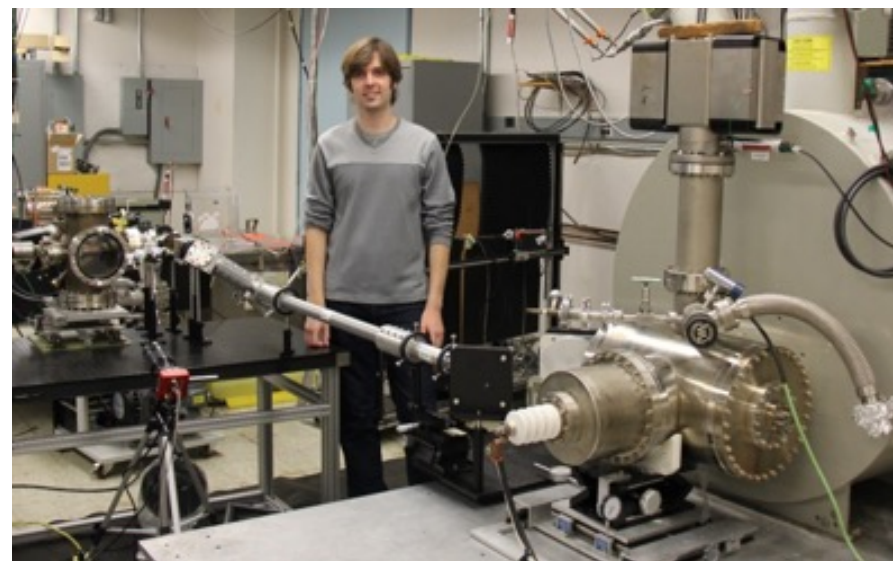
- Gyrotrons are used for Electron Cyclotron Heating (ECH) and Current Drive (ECCD) in large plasma devices in the national and international programs of fusion energy sciences, including both DIII-D and ITER. It is known that power reflection back into the gyrotron reduces the gyrotron output power and may cause changes in the gyrotron operating mode. These effects have not been studied in detail.

## Research Details

- A set of polarizing plates made of fused quartz polarize the gyrotron output beam without significant power loss. They allow completely arbitrary power reflection back to the gyrotron. Operation of the gyrotron in microsecond pulses prevents damage to the gyrotron.

## Application

These results are needed to plan major ECH/ECCD systems.



*Gyrotron Laboratory with graduate student Samuel Schaub. The gyrotron output couples directly into a corrugated waveguide, shown to the right of Mr. Schaub.*

MIT: S. Jawla, S. Schaub, M. Shapiro and R. Temkin; supported by DOE VLT

# Toward high-field compact fusion magnets: update #3 on the characterization of electro-mechanical performance of REBCO conductors

## Scientific status as of September 2018

We successfully completed the first measurement campaign on commercial REBCO tapes at 15 T and various temperatures (4.2 K to 40 K).

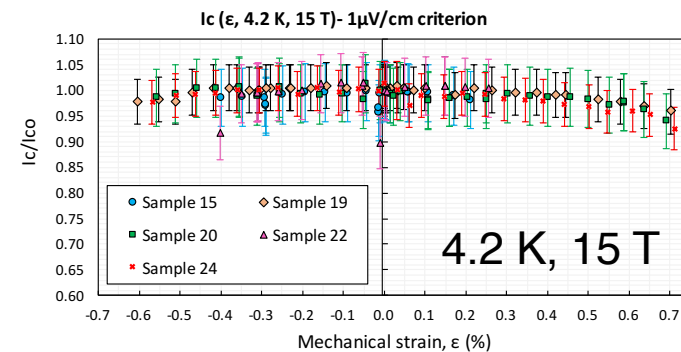
## Significance and Impact

Understanding the strain dependence at high magnetic fields and elevated temperatures (20 – 50 K) will help the design and optimization of high-current REBCO cables for high-field compact fusion reactor magnets. There are very little measurements reported in literature. We expect the ongoing study to fill this critical knowledge gap.

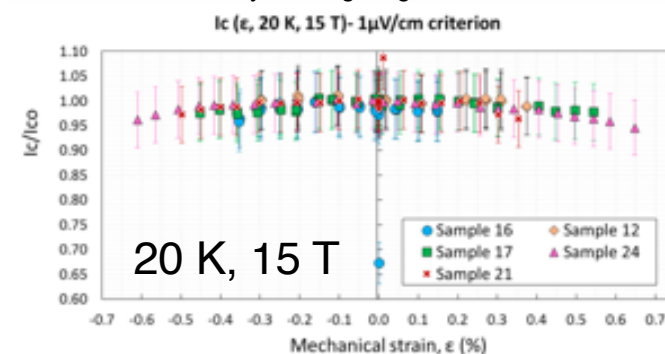
## Research Details

A first measurement campaign was completed to measure the strain dependence of commercial REBCO tapes with 30 micron thickness substrate at 20, 30 and 40 K, 15 T. Several samples were measured at each condition to obtain statistics on the strain dependence of the current carrying capability for REBCO tapes. We intend to compare the measured data with theoretical models and characterize samples from different vendors.

All samples tested showed consistent  $I_c(\epsilon)$  at 4.2 K, 15 T. Less than 5%  $I_c$  reduction (reversible) up to 0.6% compression and 0.7% tension.



A stronger strain-dependence was observed at 20 K, 15 T: ~5%  $I_c$  reduction (reversible) at 0.6% (compression or tension). Data reduction and analysis ongoing.



F. Pierro. L. Chiesa. H. Hialev. S. O. Prestemon. X. Wana

# ORNL is fabricating W-Re-Os alloys to study transmutation in W exposed to neutron irradiation

## W-Re-Os is needed by fusion material community

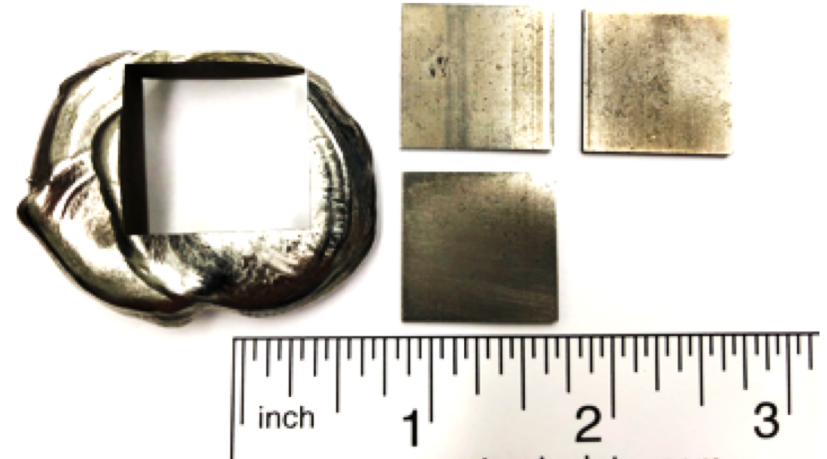
- Fusion neutron spectrum induces transmutation, converting pure W to W-Re-Os alloys in fusion reactors
- Knowledge gap exists in terms of plasma response, thermal and physical property alteration
- No available commercial W-Re-Os alloys

## Fabrication of W-5Re-3Os alloys at ORNL

- Arc melting technique
- Mixing W, W-Re, and W-Os alloys
- Chemical analysis showed 5.03wt%Re and 2.77wt%Os; GD-OES indicates the homogeneous distribution

## Use of W-Re-Os alloys

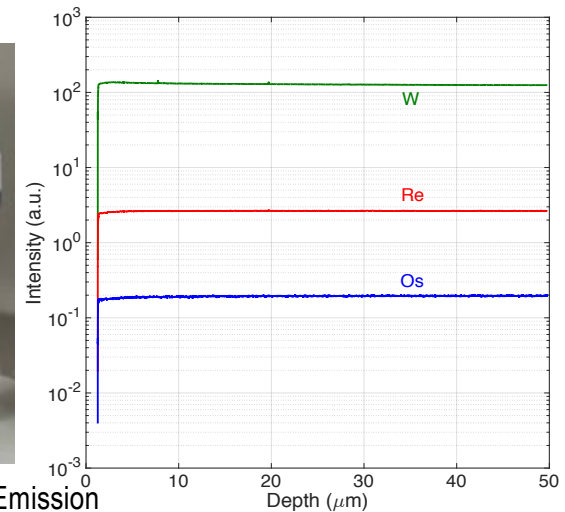
- Quantifying transmutant elements in neutron-irradiated W at ORNL
- Limited amount of W-Re-Os alloy(s) will be made available for US Fusion Materials and PMI community.
- Contact Yutai Kato (kato@ornl.gov) for inquiry and/or request.



As-fabricated W-5Re-3Os ingot and specimens prepared by using EDM



ORNL Glow Discharge-Optical Emission Spectroscopy



GD-OES elemental profile

# ORNL is using analytical tools to study the "M" side of "PMI"

## Applying modern materials science tools to:

- Analyze composition and microstructure using state-of-the-art electron microscopes
- Evaluate surface changes under high-heat-flux plasma arc lamps
- Track gas and ion implantation and release

*With the capability of handling irradiated materials*

## Fuzz characterization and mechanisms

- Microstructure of fuzz tendrils
- Detection of helium in tungsten tendrils

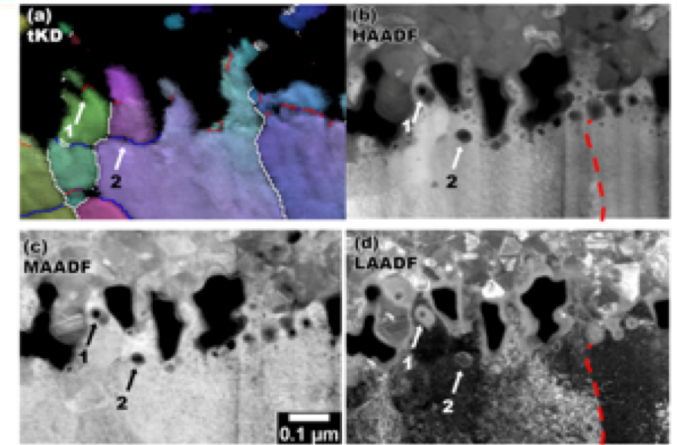
## Near surface motion, trapping, and partitioning

- Of helium and hydrogen species
- Calculating effects on the fuel cycle

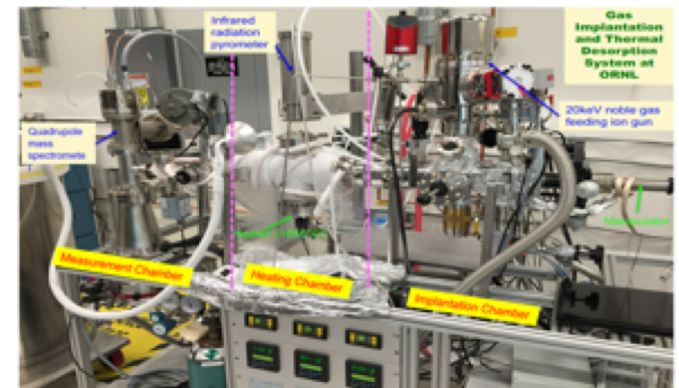
## High-heat-flux effects on divertor materials

- Cyclic HHF effects on tungsten
- Effects of prior neutron irradiation on surface response

ORNL Team: C. Parish, X. Hu, L. Garrison, A. Sabau, Y. Katoh



Nanometric analysis of fuzz-substrate interface (Wang et al., J. Nucl. Mater., 2018)

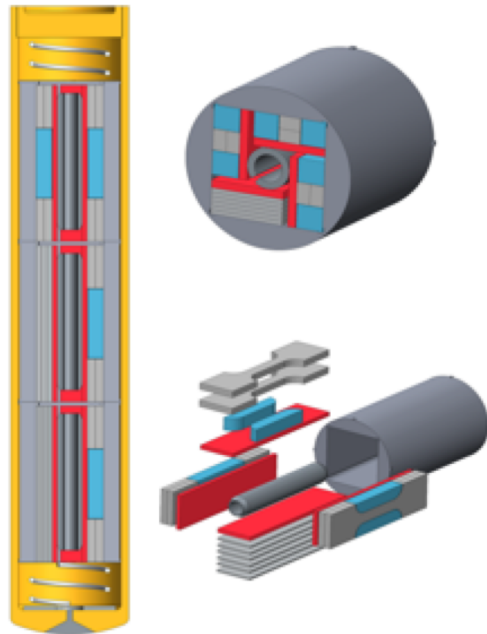


Newly developed gas analysis system in LAMDA

# Progress in the evaluation of neutron irradiation effects in EUROFER steels for KIT/EUROfusion



Specimen holder components for a HFIR tensile rabbit capsule



Schematic of assembled capsule, loaded specimen holder section, and specimen stacks ready for loading into a holder

## ORNL Contract Tasks:

1. Determine effects of 20 dpa irradiation at 220, 300 and 350°C on tensile properties and fracture toughness of EUROFER 97
2. Screen 10 EUROFER variants for 2.5 dpa irradiation at 300°C

## Experiment Design and Operation

Materials supplied by Karlsruhe Institute of Technology (KIT) as tensile and bend bar specimens

21 rabbit irradiation capsules were constructed and inserted in HFIR. Figures show typical components and schematic design

The 12-cycle HFIR Task 1 irradiations are now in the 4<sup>th</sup> cycle

The 2-cycle Task 2 irradiations are complete, capsules disassembled and samples recovered

Unirradiated materials characterized and the results reported

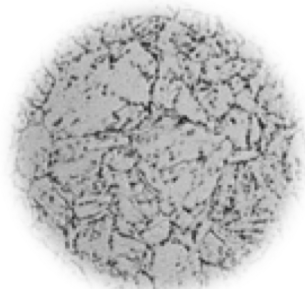
## Planned Project Completion

Task 2 specimens will be tested at ORNL during 2018

Task 1 evaluation will be determined by later negotiations

*ORNL Team: K. Linton, Y. Katoh, R. Howard, A. Bhattacharya, X. Chen*

# ORNL is evaluating several pathways to advanced steels for fusion service



OM, EUROFER 97(N&T)

## Understand RAFM Behavior

Collaborate on DEMO reference materials

- with Japan on Rad effects in F82H
- with EU (KIT), Rad effects in EUROFER97

## Cast Nanostructured Alloys

- Conventional ingot metallurgy
- High temperature strength
- Rad resistance like ODS



Cast steel in graphite mold

## Advanced Fe-base alloys

## ODS-FeCr

- Nanostructured ferritic alloy
- Higher temperature capability

Higher strength & radiation resistance

Reference base alloys

Simpler method of achieving radiation resistance

Liquid metal service

## Alumina-forming Alloys (FeCrAl)

- Enhanced corrosion resistance in PbLi



PbLi loop

Incrementally improved properties

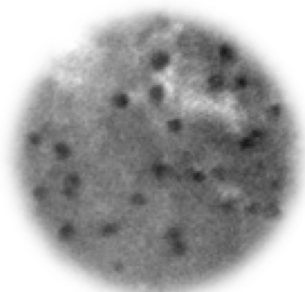
Simplified fabrication

## Advanced ODS

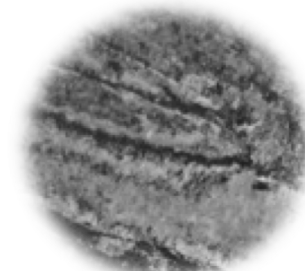
- FeCrAl with Zr mod.
  - corrosion & creep resistance
- Fe-10Cr base
  - high strength & toughness

## Bainitic Steels

- Cheaper alloying additions
- Conventional steel making
- Simplified fabrication large structures



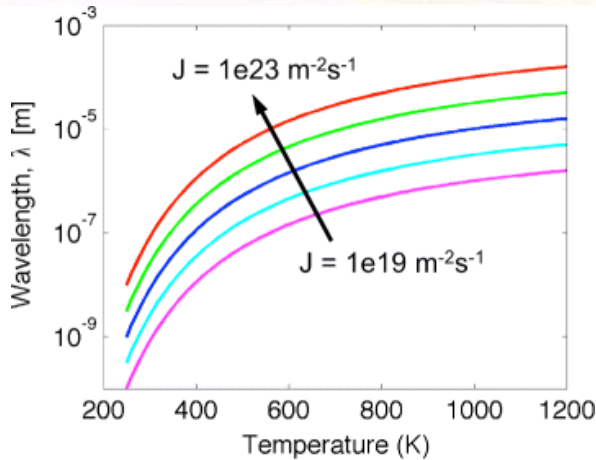
ADF-STEM, NFA 14YW7



BF-TEM, 3Cr-1.5MoV

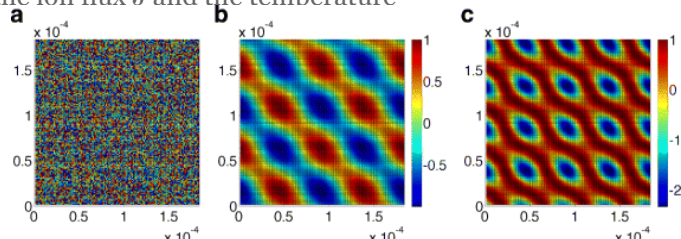
**ORNL Steel Team:** L. Tan, K. Field, Y. Yamamoto, S. Dryepontd, B. Pint, D. Hoelzer, A. Bhattacharya, Y. Katoh

# Stability and symmetry of ion-induced surface patterning



Dependence of the ripple wavelength on temperature for various incident ion flux  $J$  values, from  $10^{19}$  to  $10^{23} \text{ m}^{-2} \text{ s}^{-1}$ .  $D_0 = 2.4025 \times 10^{-7} \text{ m}^2 \text{ s}^{-1}$ ,  $\gamma = 2.9$

$[J]/[\text{m}^2 \text{ s}^{-1}]$ ,  $\Omega = 1.5825 \times 10^{-29} \text{ m}^3$ ,  $\rho_s = 7.0811 \times 10^{18} \text{ m}^{-3}$ ,  $\varepsilon = 300 \text{ eV}$ , normal ion incidence. The scale of the resulting wavelength is shown to be greatly affected by the ion flux  $J$  and the temperature



Height data for the surface profiles of the (a) original surface prior to evolution, and surface profiles after 60 h of evolution

Christopher Mattes, Nasr Ghoniem, and Daniel Walgraef Stability and symmetry of ion-induced surface patterning? *Materials Theory*, 1 (2017) 1-5..

## Scientific Achievement

The erosion of surface material by ion sputtering is a fundamental process, which leads to the formation of surface roughness and patterns at the nanoscale. The bombardment of solid surfaces with energetic ions initiates near surface collision cascades and the ejection of surface atoms. The result of such atomistic events is a complex process of roughening, pattern formation, erosion and re-deposition; all of which have the ingredients of producing pattern-forming instabilities.

## Significance and Impact

Modeling of plasma-surface interactions is a key area in the development of plasma-resilient materials for fusion energy.

## Research Details

The developed model incorporates the atomic processes of sputtering, re-deposition and surface diffusion, and is shown to display the generic features of the damped Kuramoto-Sivashinsky (KS) equation of non-linear dynamics. Linear and non-linear stability analyses of the evolution equation give estimates of the emerging pattern wavelength and spatial symmetry. The analytical theory is confirmed by numerical simulations of the evolution equation with the Fast Fourier Transform method, where we show the influence of the incident ion angle, flux, and substrate surface temperature. It is shown that large local geometry variations resulting in quadratic non-linearities in the evolution equation dominate pattern selection and stability at long time scales..



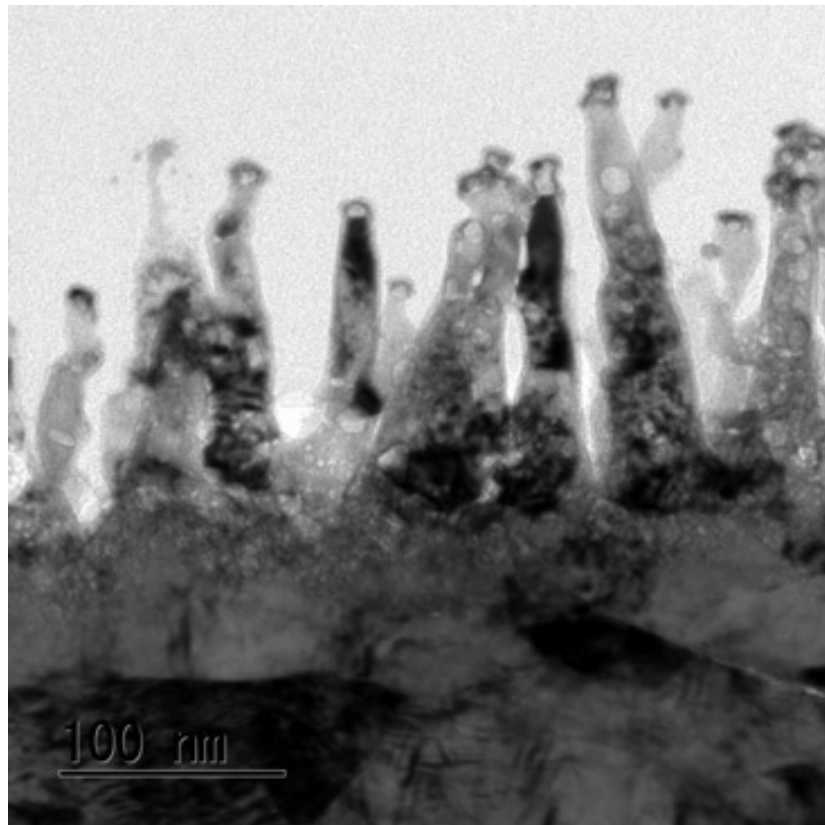
U.S. DEPARTMENT OF  
**ENERGY**

Office of  
Science

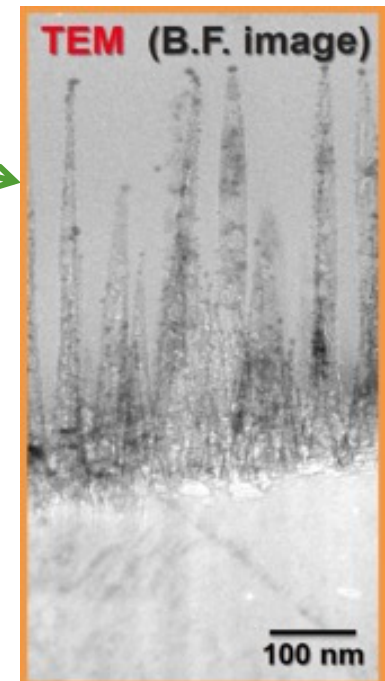


# He nano-bubble formation in plasma-exposed RAFM steel

TEM image of F82H RAFM steel after exposure to He plasma in PISCES  
 $G_i \sim 0.39 \times 10^{22} \text{ m}^{-2} \text{ s}^{-1}$ ,  $F \sim 1 \times 10^{25} \text{ m}^{-2}$ ,  
 $E_i \sim 45 \text{ eV}$ ,  $T_s \sim 573 \text{ K}$



- He bubbles form inside plasma induced surface cones in RAFM steel as well as at their bases, similar to He bubble formation in W
- W enrichment is detected at the tip of each cone
- Similar behavior is observed in pure Cr samples exposed to He plasma
- Bubbles are also observed in Be samples exposed to He plasma
- Bubbles can reduce thermal conductivity of PFCs and may cause an increase in T fuel retention
- Understanding the bubble formation conditions will help facilitate the design of more robust PFCs



# Void Formation in Self-Ion Irradiated Tungsten

## Science Objective

Object Kinetic Monte Carlo simulations predict formation of a void lattice in tungsten by one-dimensional interstitial cluster diffusion that dissociates small vacancy clusters. PKA spectrum, dose rate and grain size have significant effects in the process. This experimental study is being done to validate modeling predictions.

## Significance and Impact

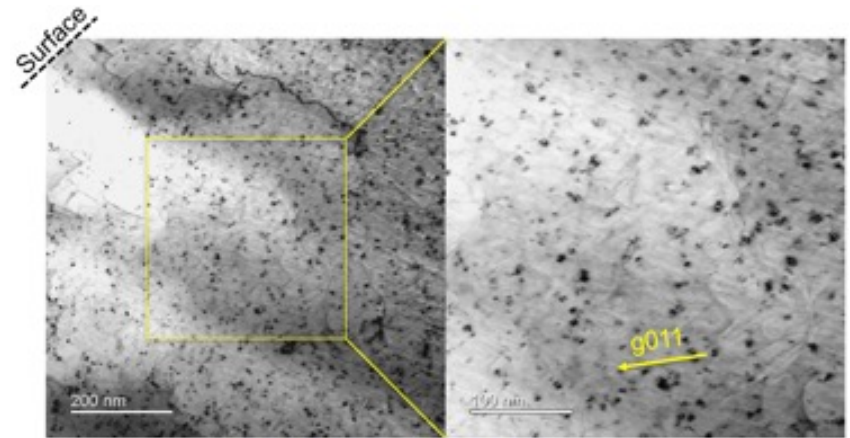
Model validation is a necessary step to successful development of predictive capabilities for microstructural evolution and property degradation in fusion materials.

## Research Details

Focused ion beam sample preparation produces black-spot defects and dislocation loops in tungsten, but not voids. A high density of voids is observed in tungsten single crystals irradiated with self-ions to 1 dpa at  $10^{-3}$  dpa/s and 900 K. Further studies are underway to observe void lattice formation in tungsten.

W. Jiana *et al.*, 2018, to be published.

Black-spot defects and dislocation loops throughout the entire cross-sectional pristine tungsten are observed, which originated from the  $\text{Ga}^+$  ion irradiation during the FIB process. Voids are not created.

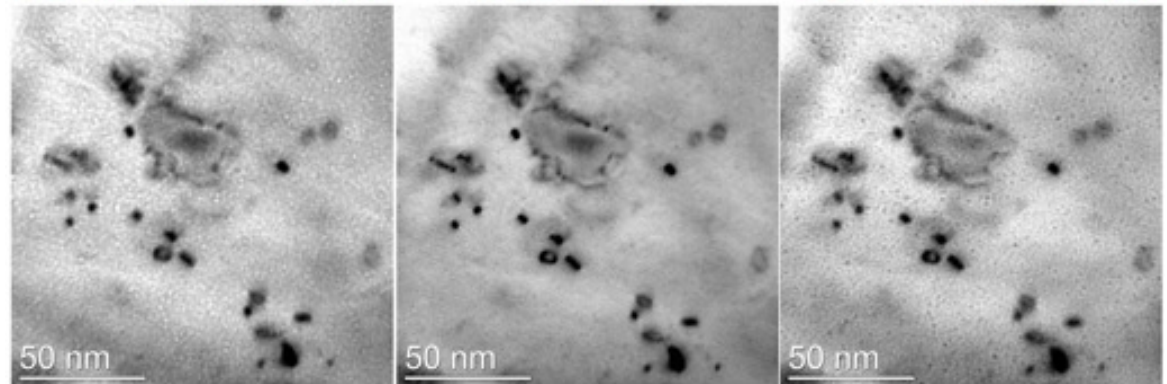


Pristine monocrystalline tungsten.

Under Focus: -1204 nm

Focus: 0 nm

Over Focus: +1204 nm



Monocrystalline W irradiated with 4 MeV  $\text{W}^{2+}$  ions to 1 dpa at  $10^{-3}$  dpa/s and 900 K; center depth:  $\sim 405$  nm.

In addition to black-spot defects and dislocation loops, a high concentration of randomly distributed voids is observed in the self-ion irradiated tungsten.

# Modeling the Effect of SIA Cluster Trapping and Detrapping on Neutron Damage in Tungsten

## Science Objective

The presence of impurities and/or minor alloying elements are known to lower irradiation-induced swelling by trapping point defects, reducing their mobility. Self-interstitial atom (SIA) clusters are preferentially trapped due to their fast diffusion relative to vacancies. Understanding the effects of SIA trapping under various irradiation conditions is needed.

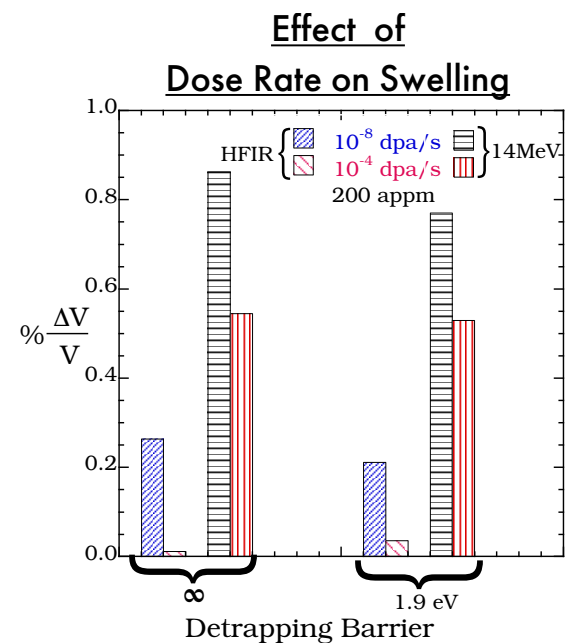
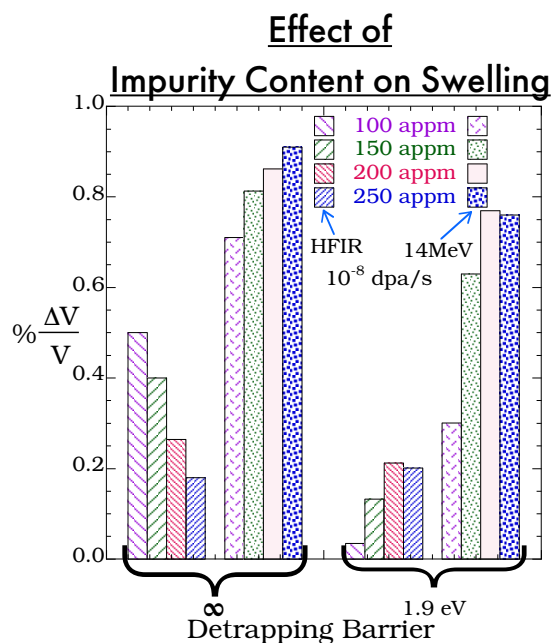
## Significance and Impact

Since no fusion neutron source exists for conducting prototypic experiments, development of predictive models of microstructure evolution under different irradiation conditions is needed to improve existing materials or to design better ones.

## Research Details

Microstructural evolution was studied using the object kinetic Monte Carlo method at various dose rates and impurity concentrations at 1025 K under HFIR and 14 MeV neutron irradiation conditions when impurities trap SIA clusters permanently or temporarily.

$\infty$  detrapping barrier  $\equiv$  SIA clusters permanently trapped



- In HFIR, swelling decreases with impurity concentration when they trap SIA clusters permanently, but not for 14MeV.
- For both irradiation conditions, swelling increases first, then decreases with impurity concentration when SIA clusters can detrapp.
- For all dose rates and impurity concentrations studied, swelling is always greater for 14 MeV than for HFIR.

- Regardless of detrapping, for both irradiation conditions, swelling increased with decreasing dose rate.
- In general, for both irradiation conditions, swelling decreases when SIA clusters are temporarily trapped.
- The efficacy of detrapping in lowering swelling is reduced with increasing dose rate (for HFIR, at 10<sup>-4</sup> dpa/s swelling increases when SIA clusters can detrapp).

G. Nandipati *et al.*, 2018, to be published.

# Kinetic-Analytic Model describing tungsten sputtering during ELMs is validated against DIII-D experimental data

## Scientific Achievement

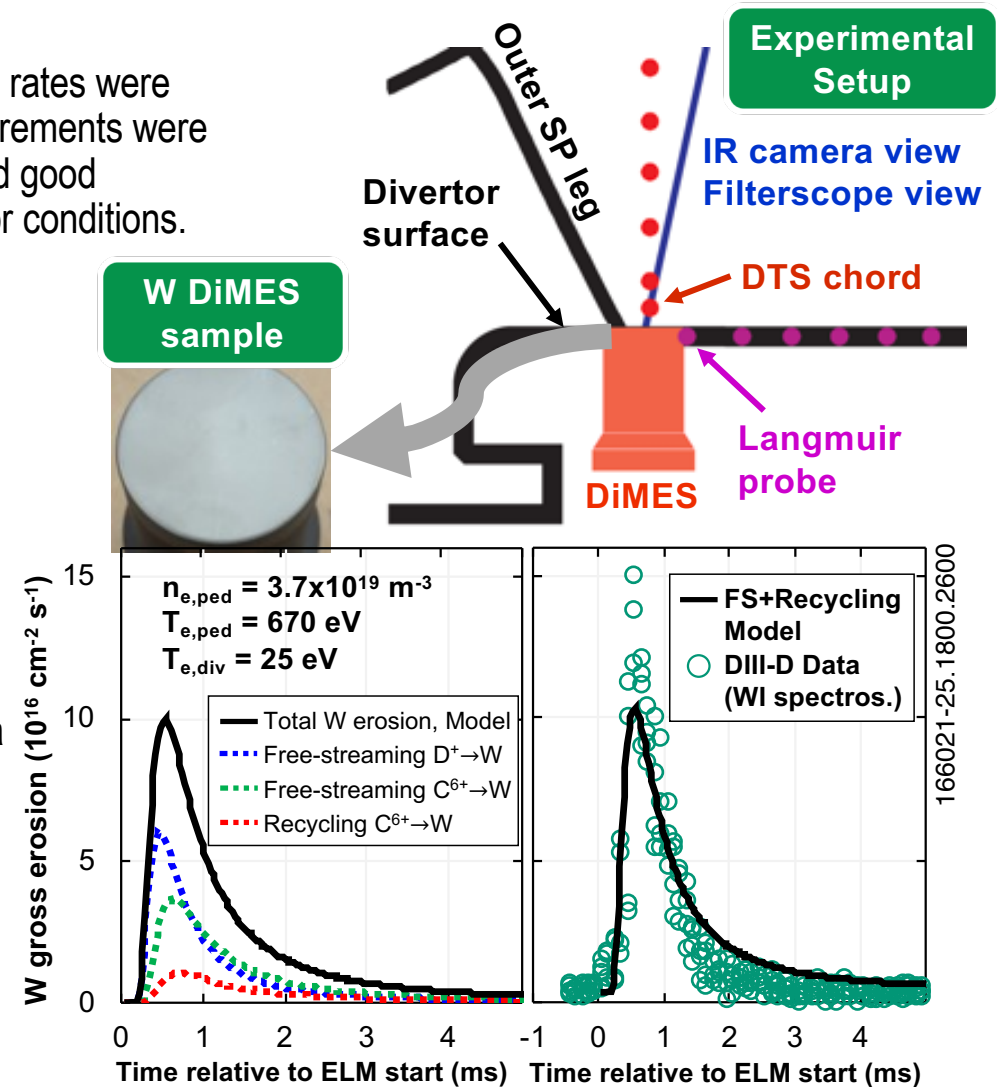
Edge Localized Mode (ELM)-resolved tungsten gross erosion rates were measured spectroscopically in the DIII-D divertor. The measurements were tested against a 1D model for ELM impacts in the divertor and good agreement was observed for a variety of pedestal and divertor conditions.

## Research Details

- 'Free-streaming' model for ELM energy/particle flux refined to include divertor recycling, good agreement with DTS/LP data.
- WI filterscope measurements acquired with high time resolution during DIII-D H-mode W DiMES exposures.
- W gross erosion inferred spectroscopically via SXB method.
- Good agreement observed between model and experimental data for a variety of divertor and pedestal conditions.
- Model predicts energetic 'free-streaming' ions from pedestal top dominate W sputtering during ELMs, despite comprising a small fraction of the ELM ion flux.

## Significance and Impact

Because ITER will operate with a partially detached divertor, it is believed that the W erosion source will be dominated by ELM events. These results suggest that it is the pedestal conditions, rather than divertor conditions, that dominate W sputtering during ELMs, underlining the need to mitigate ELM sizes in ITER to reduce W core contamination.



T. Abrams et al., Nucl. Mater. Energy 2018 (submitted)  
T. Abrams et al., APS-DPP 2018 invited (uncomin)

# Advanced Materials Modeling Used to Understand/ Improve Tungsten Recrystallization Limits

## Science Objective

Here we use molecular dynamics and multiscale modeling techniques in collaboration with the Marian group at UCLA to develop a predictive model of tungsten recrystallization.

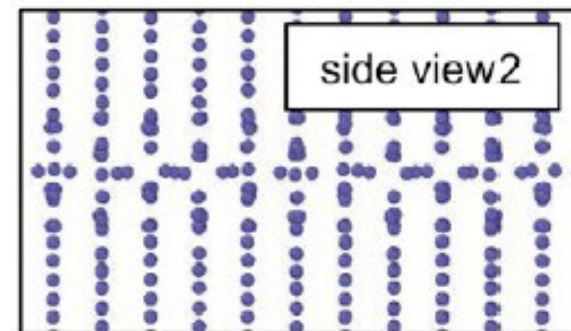
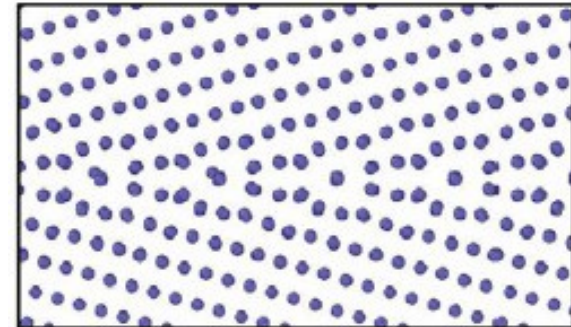
## Achievement

We predicted for the first time phase transformations in tungsten grain boundaries (GB) at high temperature. This quarter we have developed techniques to calculate grain boundary free energies across a broad range of temperatures and to calculate grain boundary mobility.

## Why it Matters

Recrystallization limits the operating temperature for tungsten and tungsten alloys in plasma facing components in tokamaks. Recrystallization involves the movement of grain boundaries in damaged metals at high temperature. It is crucial that calculations of GB properties that affect recrystallization start with the correct GB structure, something that has not been possible previously.

New Grain Boundary Structure



High-temperature structure of the tungsten  $\Sigma 27(552)[1-10]$  grain boundary ( $T = 2500\text{K}$ ) showing a new structure that forms at high temperature.

“Structures and transitions in bcc tungsten grain boundaries and their role absorption of point defects,”  
T. Frolov et al, *Acta Mater* 159, 123 (2018)

# Investigating Ceramic Breeder Thermo-mechanics Evolution with Novel Pressure Mapping Technology

## Scientific Achievement

Two modes of self-regulation were identified in a single layer ceramic breeder pebble bed thermomechanical interaction study: (1) a stress self-regulation as a result of pressure rise and fall due to thermal expansion and creep/thermal cycling, respectively, and (2) a temperature self-regulation due to the locally enhanced thermal conductivity in the core region of the bed accompanied by deteriorated interface conductance.

## Significance and Impact

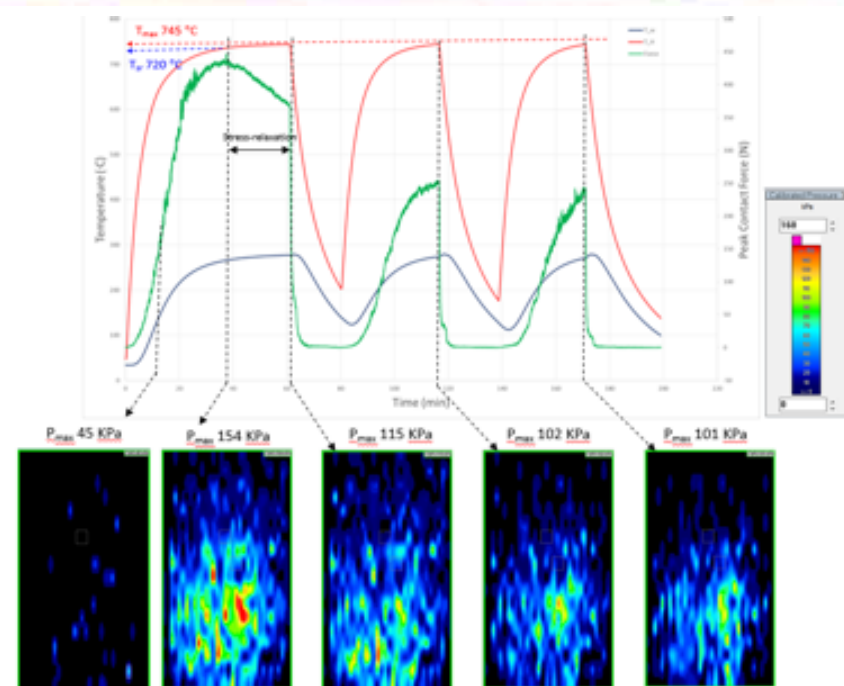
The two self-regulating mechanisms identified from the experiments are desirable as they lower the probability of the events of pebbles crushing and thermal runaways under high temperatures/stresses and poor heat extraction.

## Research Details

This study utilizes high temperature rod heaters to create a relevant nuclear temperature profile in which the pebble bed stresses are organically generated as a result of temperature gradients and magnitudes, which allows us to observe the combined thermomechanical interaction effects. A novel non-intrusive in-situ tactile pressure sensing technology is used to generate real-time contact pressure maps revealing the spatial and temporal stress evolution.

### Paper submission

Mahmoud Loffy, Alice Ying, Mohamed Abdou, Dong Won Lee, Yi-Hyun Park, Investigating Ceramic Breeder Thermo-mechanics Evolution with Novel Pressure Mapping Technology. submitted to SOFT-2018/FED



Stress and temperature evolution maps capturing the stress reduction due to creep and pebbles resettling with thermal cycling



Tactile pressure sensor calibrated in Zwick at expected temperatures and stress levels with Silica sheet and pebbles



Stress-relaxation was due to thermal creep with the pebbles necking together at high temperature core

# Understanding powder-dropper mechanisms for PFC conditioning in DIII-D should allow optimization

## Scientific Objective

The powder-dropper device has been shown to improve in-situ wall conditioning in various devices: DIII-D, EAST, and ASDEX-U. The project goal is to model dynamics of powder dispersion as it creates impurities by interactions with the edge plasma from and resulting wall-conditioning processes.

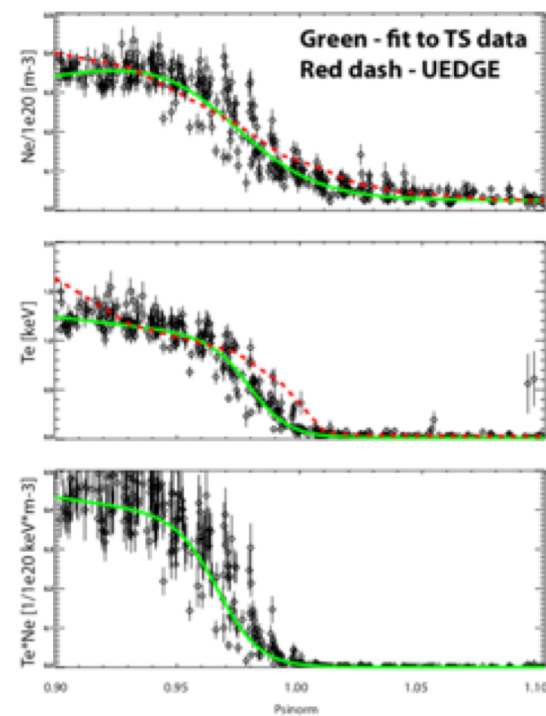
## Achievement

A multi-institution workplan is progressing to compare DIII-D powder-dropper data with modeling. Activities include experiments (PPPL), modeling powder ablation and ion deposition (LLNL & UCSD), and sheath/sputtering effects (UIUC). The initial target is DIII-D shot 175550 where the PPPL team has measured differences with discharge behavior for companion discharges where the powder-dropper is not used. Here modeling by UEDGE (right) provides the 2D boundary plasma characteristics that ablates and transports the powder, which will be followed by the DUSTT code.

## Why it matters

Wall conditioning by powder-dropping tools is a new, potentially revolutionary, techniques for real-time delivery of beneficial material (e.g., B, Li) into tokamak edge plasma; may allow run-time wall conditioning as well as advanced means for maintaining a radiative divertor.

Comparison of midplane Thomson scattering radial profiles and UEDGE simulation for DIII-D shot 175550\_3300 used for powder-dropper experiment.



# Critical Issues for Liquid PFCs include Managing Power & Particle Fluxes and Shielding Vapor

## Scientific Objective

Predict edge-plasma properties that are compatible with manageable heat flux and core plasma operation for FNSF design using liquid-metal walls. Compare results with similar configurations that used solid walls to identify key issues and impact on overall fusion performance.

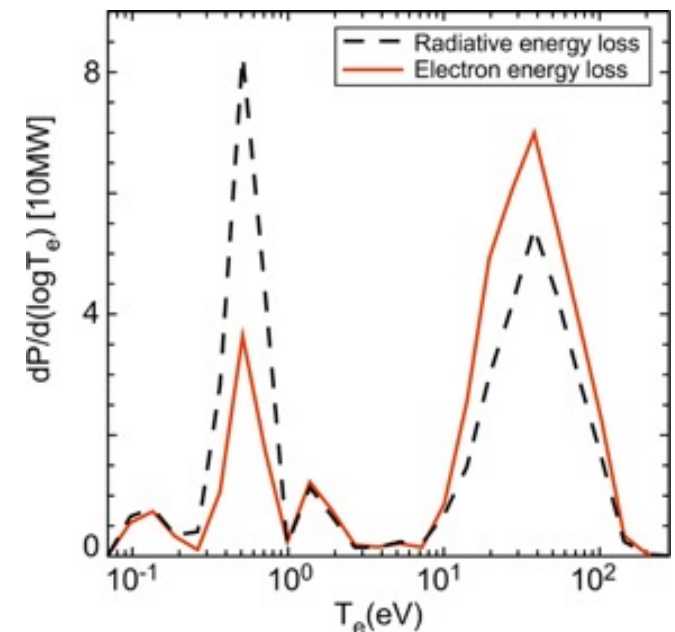
## Achievement

Continued analysis of 2D UEDGE simulations for Li divertor in FNSF geometry to understand the impact of addition shaping of the divertor target plate. Detailed analysis of numerical steady-state solutions show that the Li radiation emanates from a wide range of electron temperature regions (see right). Here the lithium radiates ~95% of the core exhaust power yielding peak heat-fluxes on wall of 2 MW/m<sup>2</sup>, a modest level.

## Why it matters

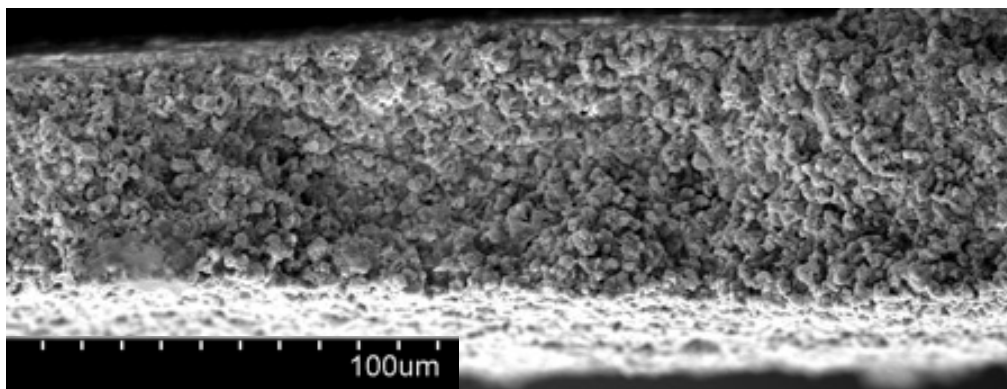
Flowing liquid walls could avoid the issue of wall erosion by ions and neutrals, and could also lead to high-performance core operational modes through high-temperature edge conditions.

Lithium divertor radiation occurs over a wide range of electron temperatures, not just low  $T_e$ . Below is energy loss spectrum vs.  $T_e$  sampled over entire divertor volume.



“Simulations of a high-density, highly-radiating lithium divertor,” T.D. Rognlien, M.E. Rensink et al. Nucl. Mat. Eng., submitted. “Study of lithium vapor flow in a detached divertor using DSMC code,” E. Emdee et al., Nucl. Mat. Eng., submitted.

# Demonstration of Direct LiT Electrolysis using an Immersion Cell



## Scientific Achievement

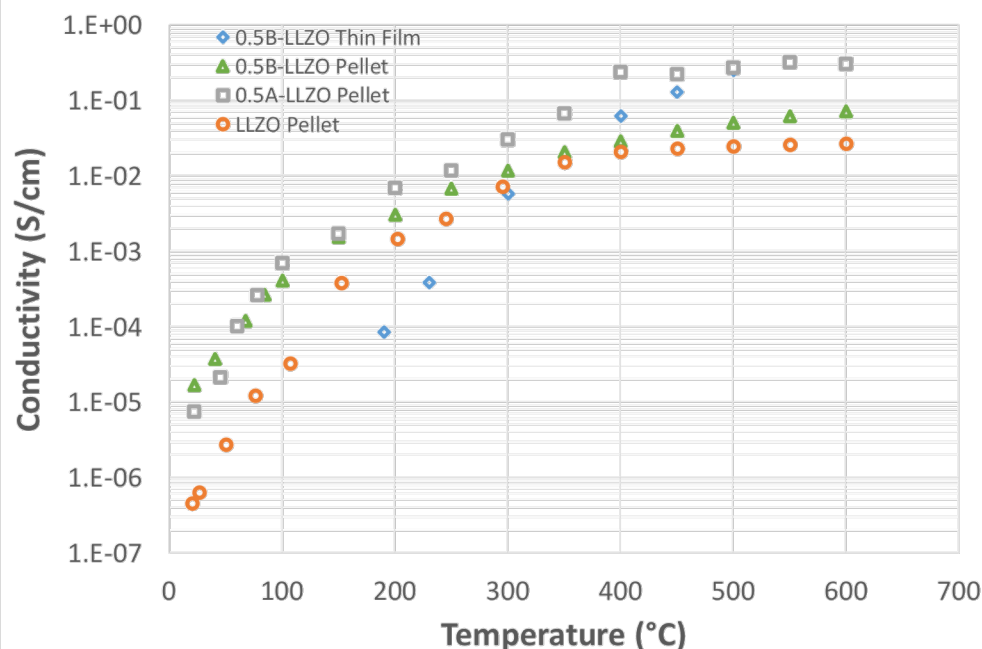
Developed and demonstrated ability to synthesize films of the electrolyte that can be used to make structurally sound electrodes with low ionic resistance

## Significance and Impact

Current techno-economic analysis for LiT electrolysis is based on having LLZO thicknesses of 50-100 microns. The ability to achieve these thicknesses with high ionic conductivity would demonstrate the viability of the electrolyte

## Research Details

- Thin-film samples with thickness less than 100 microns were able to achieve higher conductivity than pellet samples above 300° C
- Both pellets and thin film samples exceeded the target of 0.5 mS/cm at 400° C by more than a factor of 100
- The conductivity of the thin film and pellets were stable at high temperatures when cycling between 0 and 3 V, indicating stability under electrochemical operating conditions
- Results indicate that electrolyte can reach targets



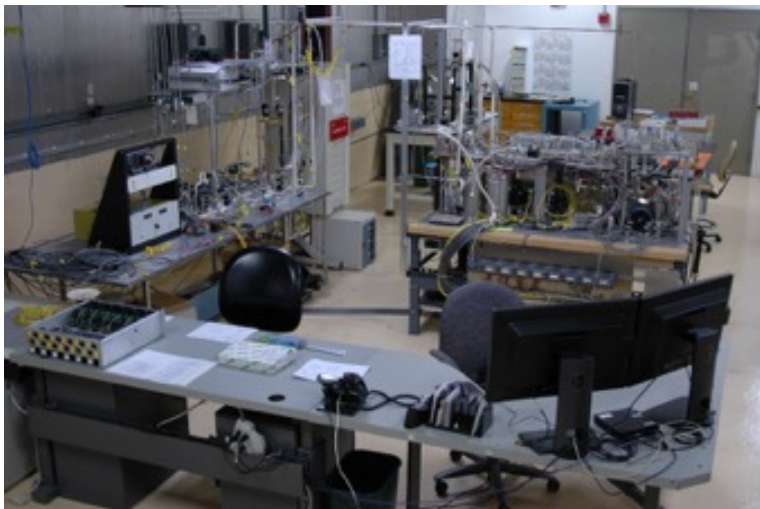
# Tritium Processing Development for Magnetic Fusion

## Application

Development and testing of tritium fuel cycle components and data-mining of TSTA historical documentation.

## Scientific Achievement

HPL system reconfigured and final wiring is underway. Developed Tritium inventory model for LM-PFC design for FNFS



Reconfigured HPL System

## Significance and Impact

- HPL and U-Bed upgrades will allow for continued engineering design development of tritium fuel cycle for fusion processes
- Integration of fuel cycle design into LM-PFC development will strengthen design options and applications.

## Research Details

- Presented preliminary model for Tritium inventory at LM-PFC Face to Face Meeting

$$\xi \approx 2S \approx \sqrt{\frac{\lambda}{a}} = \sqrt{\frac{l^2 v_0}{DL}} \quad (23)$$

For helium pumping, the value of  $\xi \approx 10^{-3} - 10^{-2}$  is small and is in the order of  $\approx 1\%$ . Fig. 2 shows the dependence of the He pumping coefficient  $\xi$  on the pumping parameter for a wide range of  $S$ .

*A Hassanein, Modeling hydrogen and helium entrapment in flowing liquid metal surfaces as Plasma-facing components in fusion designs. Journal of Nuclear Materials, 302, 2002 pg 41-48*

Hollis, W. Kirk, Victoria Hypes, LM PFC Meeting, August 2018

# Monte Carlo (MC) Variance Reduction (VR) Parameters for Shutdown Dose Rate (SDR) Calculations in Moving Systems

## Scientific Status as of Oct. 2018

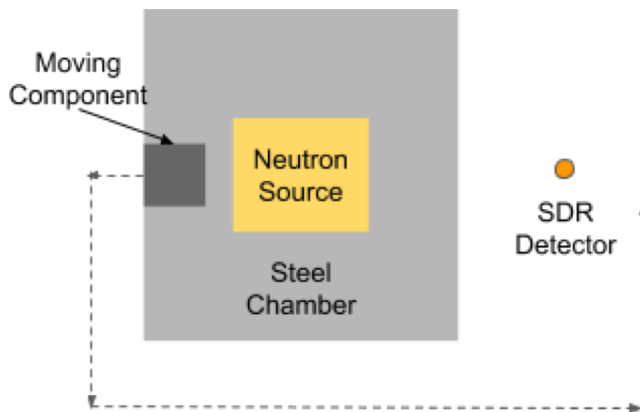
The Time-integrated Groupwise Transmutation (TGT)-CADIS method for generating MC VR parameters (biased source and weight window mesh) to optimize the neutron transport step in systems that undergo movement after shutdown has been developed and implemented.

## Significance and Impact

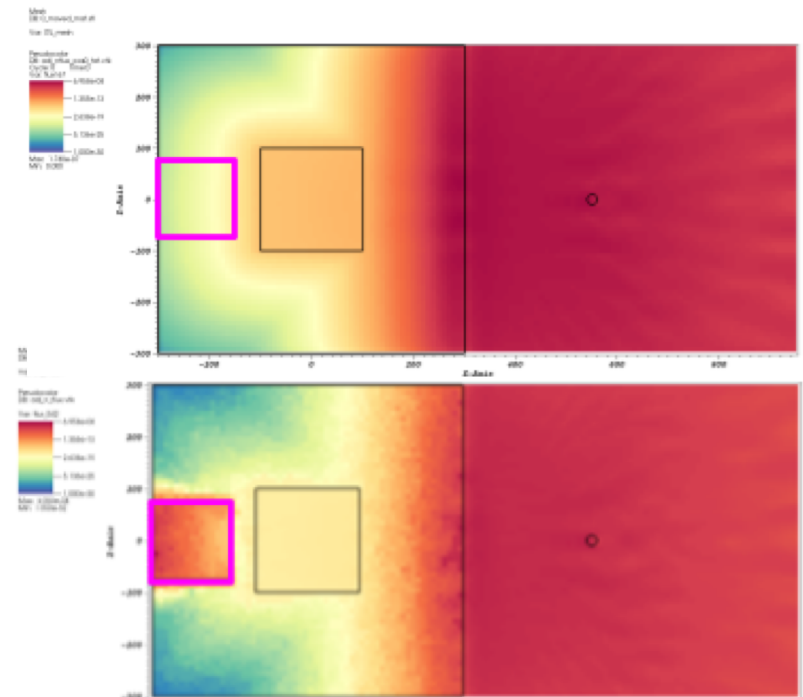
This method can be used to efficiently calculate the SDR over the time of an activated FES component moving around a facility, such as during a maintenance procedure.

## Research Details

The TGT-CADIS method generates an importance function that takes movement after shutdown into account by calculating a time-integrated adjoint neutron source.



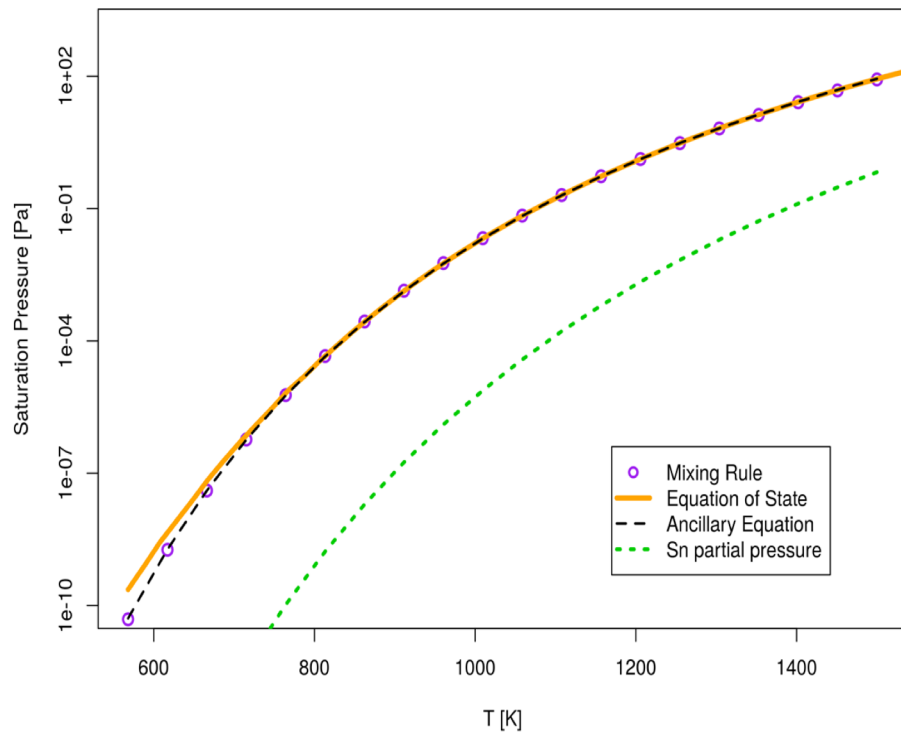
Path of activated component moving after shutdown.



Adjoint neutron flux maps produced by GT-CADIS (top) and TGT-CADIS (bottom). These represent the importance to the SDR. TGT-CADIS gives importance to the moving component, ultimately reducing statistical uncertainty in a region that will end up near the SDR detector.

UW: Chelsea D'Angelo, Paul P.H. Wilson

# A Revised and Expanded Liquid Metal Property Library for MELCOR (INL)



Paul W. Humrickhouse and Brad J. Merrill, "A Revised and Expanded Liquid Metal Property Library for MELCOR," Submitted to Fusion Engineering and Design, Sept 2018.

## Scientific Achievement

The liquid metal properties library in the MELCOR for Fusion code has been comprehensively revised. This includes a new property library implementation that simplifies the code, increases the speed of its execution, and improves the accuracy in both existing and recently added fluids.

## Significance and Impact

SnLi has been added to the MELCOR code this quarter, based on an Equation-of-States (EOS) developed to match predicted mixture properties. The code now includes the liquid metals Li, PbLi, Sn, SnLi, Na, and NaK. Liquid Li, Sn and SnLi are of interest as liquid metal plasma facing component materials.

## Research Details

Thermodynamic properties of  $\text{Sn}_{80}\text{Li}_{20}$  as a function of temperature do not seem to have been measured. We therefore estimate them using a Gibbs free energy mixing rule based on measured pure component chemical activity data and property data for saturation pressure, density, specific heat, and sound speed for Li and Sn. In order to take advantage of this predicted mixing rule data in MELCOR, a corresponding Two-Phase Helmholtz EOS had to be developed (a format required by the MELCOR EOS library) that matched these mixture data properties. Excellent agreement was achieved for saturation pressure, as seen in this figure. While not shown here, the same level of agreement was obtained for density, specific heat, and sound speed..